# Topographic Patterns of Brain Functional Impairment Progression According to Clinical Severity Staging in 116 Alzheimer Disease Patients: FDG-PET Study

*IL Han Choo, MD,* Dong Young Lee, MD, PhD,* Jong Choul Youn, MD,† Jin Hyeong Jhoo, MD, PhD,‡ Ki Woong Kim, MD, PhD,§ Dong Soo Lee, MD, PhD,‖ Jae Sung Lee, PhD,‖ and Jong Inn Woo, MD, PhD*¶*

**Abstract:** The study aimed to explore topographic progression pattern of brain functional impairment according to clinical stage in Alzheimer disease (AD). One hundred and sixteen AD patients and 25 normal subjects underwent a [$^{18}$F] fluorodeoxyglucose-positron emission tomography scan. Regional cerebral glucose metabolism was compared between severity groups based on the Clinical Dementia Rating through voxel-based analyses. As clinical severity progressed, hypometabolic areas gradually increased, involving initially posterior cingulate cortex, later temporoparietal, and finally frontal and some subcortical areas. The results indicate that progression patterns of hypometabolism in AD are close to that of typical neuropathology, but that they do not fully coincide with it.

**Key Words:** Alzheimer disease, PET, cerebral metabolism, topographic pattern

(*Alzheimer Dis Assoc Disord* 2007;21:77–84)

Alzheimer disease (AD) is the most common form of degenerative dementia and is characterized by a gradual deterioration in memory in association with other cognitive functions. Although clinical deterioration in AD seems to be basically driven by the traditionally described neuropathologic lesions of neuritic plaques and neurofibrillary tangles,[1] reductions in specific neuron and synapse populations have also been associated with functional decline.[2–4]

Cerebral glucose metabolism, as measured by positron emission tomography (PET) with [$^{18}$F] fluorodeoxyglucose (FDG), is a reliable index of neuronal or synaptic activity[5,6] and earlier FDG-PET studies on AD have frequently demonstrated global brain hypometabolism. Moreover, characteristic patterns of regional hypometabolism predominantly involve associative posterior and frontal areas whereas primary cortices are relatively spared.[7–11] Some reports also indicate that the range of metabolic reduction tends to extend in temporoparietal or frontal areas as the clinical severity of dementia progresses.[7,11,12] A series of recent functional imaging studies on AD patients with very mild stage or mild cognitive impairment (MCI) have shown that hypometabolism or hypoperfusion occur at the posterior cingulate cortex (PCC).[13–15]

However, our understandings on clinical severity-specific, detailed topographical pattern of glucose hypometabolism in the whole brain of AD patients is not sufficient yet, which seems to be related to some methodologic limitations in previous studies on this issue. Most of these earlier studies relied on visual inspection[11] or region of interest (ROI) methods.[7,11] Although the ROI approach is a useful technique, it only focuses on selected areas, thus many brain regions may be left unexplored. Although a study[14] did adopt a voxel-based approach to reveal the severity-related pattern of metabolism in AD, it explored only for cortical brain areas, but not for subcortical areas. Furthermore, most previous studies on this issue adopted the Mini-Mental State Examination (MMSE)[16] as a clinical severity measure. Although MMSE has been widely used as a severity measure for AD or dementia, it has some critical limitations in reflecting the severity of AD patients. It has a floor effect for severe dementia cases and loses its discriminability for disease progression as the severity of the illness increases. It has also been criticized for its poor reflection on the right hemisphere and frontal lobe-related cognitive function.[17] Additionally, the number of subjects enrolled in previous studies was relatively small[7,11,12] or in some cases subjects at certain stages of clinical severity were even not included.[7,11]

Received for publication June 20, 2006; accepted March 20, 2007.

From the *Department of Neuropsychiatry and Clinical Research Institute; ‖Department of Nuclear Medicine; ¶Neuroscience Research Institute of the Medical Research Center, Seoul National University, Seoul; †Department of Neuropsychiatry, Kyunggi Provincial Hospital for the Elderly, Yongin; §Department of Neuropsychiatry, Seoul National University Bundang Hospital, Seongnam, Kyunggi; and ‡Department of Psychiatry, Kangwon National University Hospital, Chuncheon, Kangwon, Korea.

Supported by the Seoul National University Hospital Research Fund (Grant No. 04-98-045) and the "Biotech 2000" program of the Korean Ministry of Science and Technology (Grant Nos. 97-N1-02-03-A-12 and 98-N1-02-03-A-12).

Reprints: Jong Inn Woo, MD, PhD, Department of Neuropsychiatry, Seoul National University Hospital, 28 Yongon-dong, Chongno-gu, Seoul, 110-744, Korea (e-mail: jiwoomd@plaza.snu.ac.kr).

In this study, we aimed to explore the clinical severity-specific regional distribution patterns of decreased glucose metabolism for a large number of AD patients in very mild to severe stage through voxel-based analysis covering entire brain areas. We used the Clinical Dementia Rating (CDR)[18] as a clinical severity index, instead of MMSE. CDR, based on clinical judgment through an extensive clinical interview, does not have a floor effect for progressed AD cases and is more appropriate for the assessment of the clinical severity or stage of AD. Correlation between regional glucose metabolism and AD severity was also examined on a voxel by voxel basis.

## METHODS

### Subjects

Subjects were recruited from a cohort of AD patients regularly followed at the Dementia and Age-associated Cognitive Decline Clinic at Seoul National University Hospital. One hundred and sixteen AD patients were included after a standardized clinical assessment and neuropsychologic testing as described below. All the AD subjects included in this study met both the Diagnostic and Statistical Manual of Mental Disorders (DSM-IV) criteria for dementia[19] and the National Institute of Neurological and Communication Disorders and Stroke/Alzheimer's Disease and Related Disorders Association (NINCDS-ADRDA) criteria for probable AD.[20] AD patients were classified into 4 severity groups according to the CDR scores, that is, very mild AD (CDR 0.5; n = 35), mild (CDR 1; n = 46), moderate (CDR 2; n = 27), and severe (CDR 3; n = 8). Twenty-five age-matched healthy normal controls (NC: CDR 0) were also selected from a pool of volunteers with a normal neurologic and psychiatric history and examination, and a normal brain magnetic resonance imaging (MRI).

The study exclusion criteria were any present serious medical, psychiatric, or neurologic disorder that could affect mental function; evidence of a focal brain lesion on MRI; the presence of severe behavioral or communication problems that would make a clinical or PET examination difficult; ambidextrousness or left-handedness; and an absence of a reliable informant.

The Institutional Review Board of Seoul National University Hospital approved the study protocol and informed consent was obtained from all study subjects and their relatives.

### Clinical and Neuropsychologic Assessments

All subjects were examined by neuropsychiatrists with advanced training in neuropsychiatry and dementia research according to the protocol of the Korean Version of the Consortium to Establish a Registry for Alzheimer's Disease Assessment Packet (CERAD-K).[21,22] Psychiatric, general physical, and neurologic examinations; routine laboratory tests; MRI of the brain; and 8 neuropsychologic tests (Verbal fluency, 15-item Boston naming test, MMSE, Word list memory, Word list recall, Word list recognition, Constructional praxis, Constructional recall) included in CERAD-K were performed. A panel consisting of 4 neuropsychiatrists with expertise in dementia research made clinical decisions, including the assignment of CDR rating. Two psychiatrists (D.Y.L. and K.W.K.) included in the panel had completed the CDR training course run by the Washington University Alzheimer's Disease Research Center and were certificated as CDR raters. CDR Sum of Boxes (CDR-SOB)[23] scores were calculated by summing ratings across the 6 functional domains of the CDR and used as an additional quantitative variable of functional severity in each individual. All clinical assessments were carried out within 4 weeks of PET examination.

### PET Imaging

PET studies were performed using an ECAT EXACT 47 scanner (Siemens-CTI, Knoxville, TN) with an intrinsic resolution of a 5.2 mm full width at half maximum and 47 contiguous transverse plane images with a 3.4-mm thickness for a longitudinal field of view of 16.2 cm. Before administering FDG, transmission scanning was performed, using 3 germanium-68 rod sources to correct attenuation. Static emission scans began 30 minutes after the intravenous injection of 370 MBq (10 mCi) FDG and were continued for 30 minutes. All FDG-PET scans were performed in a dimly lit room with minimal auditory stimulation during both injection and PET scanning, with a subject in the supine position with their eyes closed to minimize confounding effects due to any activity. Transaxial images were reconstructed using a filtered back-projection algorithm employing a Shepp-Logan filter with a cutoff frequency of 0.3 cycles/pixel and $128 \times 128 \times 47$ matrices of size of $2.1 \times 2.1 \times 3.4$ mm.

### PET Data Analysis

Imaging data were analyzed using Statistical Parametric Mapping (SPM) 99 (Institute of Neurology, University College of London, UK) implemented in the Matlab (Mathworks Inc, USA). Before statistical analysis, all images were spatially normalized to the Montreal Neurological Institute (MNI, McGill University, Montreal, CA) space to correct intersubject anatomic variabilities. An affine transformation was performed to determine the 12 optimal parameters essential for registering the brain on the MNI template. Subtle differences between transformed images and the template were removed by a nonlinear registration method using the weighted sum of predefined smooth basis functions used in a discrete cosine transformation. Using an in-house Matlab-based program, the glucose metabolism value of each voxel was normalized versus pontine value, which was extracted for each scan, because glucose metabolism in the pons tends to be relatively preserved in AD.[24] In this program, the volume of interest for the pons was predefined in the MNI space and applied to the individual spatially normalized PET images to measure the mean pontine activity. Normalized images were smoothed by convolution using an isotropic

Gaussian kernel with 16 mm full width at half maximum to accommodate intersubject differences in gyral and functional anatomies and to increase dataset signal-to-noise ratios.

Differences in glucose metabolic values between any 1 of the 4 AD severity groups and NC group, and between any 2 AD severity groups, were estimated on a voxel-by-voxel basis using the *t* statistic. The resulting set of *t* values constituted the SPM(t) map. The SPM(t) was then transformed to the unit normal distribution to give a SPM(Z).[25] In SPM analysis for functional imaging data, to render the chance probability of finding over the entire SPM suitably small (eg, 0.05), 2 types of threshold for making a statistical inference about any observed regional effect are used: (1) a critical height that the region has to reach (height threshold), (2) a critical size above some threshold that a region must exceed before it is considered significant (cluster size threshold). Another way of looking at this is to consider that a local excursion of the SPM (a connected or contiguous subset of voxels above some threshold) can be characterized by its maximal value (*Z*) or by its size (the number of voxels that constitutes the region). These 2 thresholds form the basis for making a statistical inference about any observed regional effect.[25] We applied both *P* value $< 0.001$ (uncorrected for multiple comparisons: *Z* score $> 3.09$) as a significance height threshold and 25 voxels as a cluster size threshold to decrease the probability of detecting false positives.[26,27] As for another direction of multiple comparisons related to the comparison between any 2 severity groups, we did not apply any correction to control type I errors because we aimed not to confirm, but to just explore the regional distribution patterns of glucose metabolic reduction without a priori hypotheses. Correlation between glucose metabolism and CDR-SOB score was also analyzed on a voxel-by-voxel basis for AD patients. For this correlation analysis, ''single-subject: covariates only'' module in SPM was applied and age was adjusted in the correlation analysis by using ''nuisance variable'' menu in SPM (ie, partial correlation was analyzed) because many previous studies indicate that age significantly affects regional glucose metabolism or perfusion.[28,29,30] On the basis of our results of group comparisons and previous reports on the hypometabolic brain areas in AD,[8,10,14,26] we hypothesized that glucose metabolism in the posterior cingulate or temporoparietal cortex is correlated with CDR-SOB scores. For these specific areas, therefore, a significance height threshold of $P < 0.005$ (uncorrected) was applied to test the significance of correlations. A cluster size threshold of 25 voxels was also applied. The MNI coordinates of the local maximum of each voxel cluster were automatically calculated in SPM, and it can be transformed to Talairach coordinates[31] by ''min2tal'' program (ftp://ftp.mrc-cbu.cam.ac.uk/pub/imaging/MNI2tal/mni2tal.m).

## Demographic and Clinical Data Analysis

Differences across the groups with respect to demographic and clinical variables were tested by analysis of variance or $\chi^2$ tests. All analyses were performed using SPSS software, version 10.0. (SPSS Inc, USA)

# RESULTS

The demographic and clinical characteristics for NC and each AD severity group are shown in Table 1. Age and education were not significantly different across all 5 groups. Although female ratio in the CDR 3 group was significantly lower than that in the CDR 0.5 group ($\chi^2 = 4.85$, $df = 1$, $P = 0.028$), there was no significant sex difference between other paired groups. CDR-SOB scores and T-scores of each cognitive test, on the basis of normative data of healthy Korean elderly people,[32] were significantly different across all 5 groups by analysis of variance and the results from Turkey post hoc comparison are shown in Table 1.

When compared with the NC group (CDR 0), each of the AD severity groups showed reduced glucose metabolism in the following brain regions: only PCC for very mild AD (CDR 0.5); PCC, anterior cingulate cortex, bilateral temporal cortex, and left thalamus for mild AD (CDR 1); PCC, left temporal cortex and bilateral inferior parietal cortex for moderate AD (CDR 2); bilateral frontal cortex, diffuse temporal and parietal cortex, right thalamus and right caudate for severe AD (CDR 3) (Table 2; Fig. 1). When any adjacent 2 among the 4 AD severity groups were compared, there were no significant metabolic differences between CDR 0.5 and CDR 1, and between CDR 1 and CDR 2, whereas the CDR 3 group showed significantly lower glucose metabolism in left parahippocampal gyrus, left middle temporal gyrus, and left inferior frontal gyrus, than the CDR 2 group. The CDR 3 group also showed significantly reduced metabolism in right PCC and right inferior parietal lobule compared with the CDR 0.5 group, and left temporal fusiform gyrus compared with the CDR 1 group (Table 2). Although not statistically significant, the CDR 2 group showed relative hypometabolic tendency in the PCC [0, −34, 27, $Z = 2.84$, Brodmann area (BA) 31] and right inferior parietal cortex (57, −50, 39, $Z = 2.71$, BA 40), when compared with the CDR 0.5 group ($P < 0.005$, uncorrected).

A significant negative correlation between CDR-SOB and glucose metabolism was found in right PCC (6, −36, 28, $Z = 2.72$, BA 23), right inferior parietal lobule (57, −50, 39, $Z = 3.05$, BA 40), and left inferior parietal lobule (−46, −58, 42, $Z = 2.68$, BA 40) in all 116 AD patients (Fig. 2). Normalized metabolism value was extracted at the local maximum of each voxel cluster showing significant correlation using voxel of interest module of SPM to estimate the degree of correlation between CDR-SOB and glucose metabolism. Pearson correlation coefficient (*r*) was −0.27 for right PCC, −0.26 for right inferior parietal lobule, and −0.25 for left inferior parietal lobule ($P < 0.01$ for each of the correlations). Figure 3 illustrates the correlation between CDR-SOB score and normalized glucose metabolism at PCC in AD.

**TABLE 1.** Demographic and Clinical Characteristics of the Study Subjects

| | CDR 0 NC (n = 25) | CDR 0.5 AD (n = 35) | CDR 1 AD (n = 46) | CDR 2 AD (n = 27) | CDR 3 AD (n = 8) |
|---|---|---|---|---|---|
| Age (y) | 70.0 ± 7.3* | 70.0 ± 6.9 | 69.5 ± 8.4 | 68.5 ± 10.7 | 65.6 ± 9.6 |
| Age at onset (y) | — | 66.8 ± 7.2 | 66.0 ± 8.8 | 65.9 ± 10.7 | 61.6 ± 11.5 |
| Education (y) | 8.4 ± 5.7 | 7.5 ± 5.1 | 7.2 ± 5.9 | 7.3 ± 5.9 | 8.0 ± 5.0 |
| Sex (female %) | 56.0 | 77.1 | 71.7 | 70.4 | 37.5† |
| CDR-SOB score‡ | 0.0 ± 0.0 a | 3.3 ± 0.6 b | 5.9 ± 1.5 c | 11.1 ± 1.8 d | 16.9 ± 0.8 e |
| Cognitive test score | | | | | |
| Word fluency‡ | 56.9 ± 10.0 a | 39.8 ± 8.7 b | 34.7 ± 8.8 b | 28.5 ± 10.4 b, c | 12.6 ± 5.4 c |
| 15-item Boston naming‡ | 54.9 ± 7.7 a | 42.8 ± 10.5 a, b | 38.2 ± 13.5 a, b | 38.4 ± 25.1 a, b | 22.3 ± 7.8 b |
| Mini-Mental State‡ | 51.9 ± 8.5 a | 23.7 ± 19.2 b | 12.7 ± 22.7 b, c | − 3.3 ± 36.2 c | − 53.2 ± 21.1 d |
| Word list memory‡ | 55.1 ± 7.6 a | 30.7 ± 9.8 b | 28.8 ± 11.5 b | 23.5 ± 14.0 b, c | 4.4 ± 9.5 c |
| Constructional praxis‡ | 57.8 ± 5.5 a | 42.6 ± 9.4 a, b | 44.5 ± 18.6 a, b | 27.7 ± 30.4 b, c | 15.1 ± 20.5 c |
| Word list recall‡ | 56.1 ± 7.8 a | 27.0 ± 7.3 b | 26.5 ± 9.1 b | 25.1 ± 8.1 b | 21.2 ± 4.8 b |
| Word list recognition‡ | 51.9 ± 6.6 a | 19.1 ± 19.6 b | 16.4 ± 18.6 b, c | 15.9 ± 17.4 b, c | − 3.8 ± 16.8 c |
| Constructional recall‡ | 57.1 ± 9.5 a | 34.1 ± 6.5 b | 33.2 ± 9.1 b | 34.6 ± 8.9 b | 29.8 ± 5.5 b |

All cognitive test scores are age, education, and sex-specific norm corrected T-score.
*Mean ± SD.
†Significantly different ($P < 0.05$) by $\chi^2$ test, compared with CDR 0.5 AD group.
‡Significant overall group differences found ($P < 0.001$) by analysis of variance: The alphabets below the scores indicate statistically different groups identified in post hoc comparisons by Turkey method.

## DISCUSSION

This study describes topographic progression patterns of glucose utilization deficit across the clinical severity spectrum of AD from very mild to severe stage disease. Compared with the NC, very mild AD patients showed reduced glucose metabolism only in the PCC. As clinical severity progressed from mild to severe, the extent of hypometabolism in the PCC and temporoparietal cortex gradually increased. In severe stage disease, additional bilateral frontal and even subcortical hypometabolism was also found. Although significant metabolic differences were not always observed between any 2 of the 4 AD severity groups, similar increasing patterns of reduced metabolic areas from very mild to severe AD groups were also indicated from interseverity group comparisons. To the best of our knowledge, this is the largest cross-sectional, voxel-based FDG-PET study on the relationship between clinical severity and regional hypometabolism pattern in AD to date.

One previous study reported that glucose hypometabolism initially appeared in bilateral superior and medial parietal cortices in mild stage disease and then progresses to frontal and temporal areas.[7] Another study reported a glucose metabolism decline in parietal and lateral temporal cortices in mild stage AD, in parietal and premotor cortices in moderate AD, and in all regions except the occipital lobes in severe AD.[33] However, these reports were based on ROI analyses and could not demonstrate stage-specific hypometabolism patterns across the whole area of brain including subcortical areas. Minoshima et al[14] explored the relationship between MMSE score, as a clinical severity measure, and metabolic decline in AD through voxel-based analyses using a 3-dimensional stereotactic surface projection technique (3D-SSP) and revealed that metabolic reduction initially involved PCC in the very mild stage of AD and progressed to temporoparietal and then frontal cortex. Although our results basically confirm those of Minoshima et al,[14] we additionally revealed severity-related metabolic decline in subcortical brain areas, such as thalamus and caudate nucleus. Whereas SPM method used in our study can cover subcortical areas and cortical brain regions, 3D-SSP extracts data only from cortical areas. This limitation of 3D-SSP, compared with SPM, could explain why subcortical metabolic decline was not detected in the study of Minoshima et al.[14]

Thalamic hypometabolism was observed even in the mild stage, while the caudate was not involved until the severe stage. One voxel-based PET study previously reported caudate and thalamic hypometabolism especially in early onset AD.[34] Another PET study showed metabolic reduction in the medial thalamus and mamillary bodies.[15] An MRI volumetric study also showed thalamic atrophy in AD,[35] and some histopathologic studies have described changes in the thalamus and caudate in AD.[36,37] Our results indicate that subcortical hypometabolism, like cortical hypometabolism, may

**TABLE 2.** Brain Areas Showing Significant Hypometabolism in Comparisons Between Paired CDR Groups

| Comparisons | Regions | BA | Coordinates (mm) | | | Z value |
|---|---|---|---|---|---|---|
| | | | X | Y | Z | |
| CDR 0.5 vs. CDR 0 | Right PCC | 23 | 6 | −38 | 24 | 3.46 |
| CDR 1 vs. CDR 0 | Left PCC | 23 | −2 | −32 | 26 | 4.69 |
| | Right anterior cingulate cortex | 24 | 4 | 15 | 23 | 3.62 |
| | Right inferior temporal gyrus | 20 | 63 | −34 | −17 | 3.68 |
| | Left superior temporal gyrus | 22 | −48 | 13 | −9 | 3.39 |
| | Left thalamus | — | −4 | −17 | 12 | 3.50 |
| CDR 2 vs. CDR 0 | Right PCC | 23 | 2 | −36 | 26 | 4.73 |
| | Left middle temporal gyrus | 20 | −55 | −40 | −13 | 4.51 |
| | Left inferior parietal gyrus | 40 | −48 | 58 | 40 | 4.21 |
| | Right supramarginal gyrus | 40 | 57 | −53 | 36 | 3.61 |
| | Right inferior parietal cortex | 40 | 50 | −56 | 43 | 3.55 |
| CDR 3 vs. CDR 0 | Left inferior temporal gyrus | 20 | −55 | −38 | −18 | 6.37 |
| | Right inferior temporal gyrus | 20 | 63 | −22 | −16 | 5.97 |
| | Right angular gyrus | 39 | 51 | −57 | 34 | 5.38 |
| | Left inferior parietal lobule | 40 | −53 | −50 | 43 | 5.19 |
| | Right superior temporal gyrus | 22 | 59 | −50 | 15 | 5.14 |
| | Left uncus | 20 | −36 | −11 | −33 | 5.09 |
| | Right posterior cingulate gyrus | 23 | 6 | −41 | 30 | 4.92 |
| | Left medial frontal gyrus | 25 | −8 | 7 | −17 | 4.78 |
| | Left superior temporal gyrus | 38 | −36 | 10 | −34 | 4.53 |
| | Left inferior temporal gyrus | 20 | −32 | −6 | −37 | 4.67 |
| | Right uncus | 20 | 28 | −15 | −28 | 4.42 |
| | Right anterior cingulate cortex | 24 | 2 | 11 | 23 | 4.26 |
| | Left superior frontal gyrus | 8 | −18 | 28 | 54 | 3.72 |
| | Left middle frontal gyrus | 11 | −44 | 44 | −11 | 3.98 |
| | Left inferior frontal gyrus | 10 | −42 | 52 | 1 | 3.86 |
| | Right superior frontal gyrus | 8 | 8 | 41 | 48 | 3.51 |
| | Right middle frontal gyrus | 9 | 48 | 27 | 35 | 3.34 |
| | Right thalamus | — | 12 | −17 | 17 | 3.55 |
| | Right caudate | — | 14 | 10 | 9 | 3.46 |
| CDR 3 vs. CDR 0.5 | Right posterior cingulate gyrus | 31 | 4 | −39 | 30 | 3.68 |
| | Right inferior parietal lobule | 40 | 51 | −55 | 43 | 3.22 |
| CDR 3 vs. CDR 1 | Left temporal fusiform gyrus | 20 | −48 | −25 | −26 | 3.13 |
| CDR 3 vs. CDR 2 | Left parahippocampal gyrus | 34 | −14 | −5 | −17 | 4.55 |
| | Left middle temporal gyrus | 21 | −53 | −8 | −11 | 3.40 |
| | Left inferior frontal gyrus | 47 | −44 | 17 | −3 | 3.18 |

CDR 0 indicates NC (n = 25); CDR 0.5, very mild AD patients (n = 35); CDR 1, mild AD patients (n = 46); CDR 2, moderate AD patients (n = 27); CDR 3, severe AD patients (n = 8).

Coordinates, anatomic area, and estimated BA are from Talairach and Tournoux.[30] X is the distance in mm to the right (+) or left (−) of midline; y is the distance anterior (+) or posterior (−) to the anterior commissure, and z is the distance superior (+) or inferior (−) to a horizontal plane through the anterior and posterior commissure.

progress according to a specific pattern or sequence, and initially involve the thalamus and then the caudate nucleus in AD.

Although the topographic progression patterns of regional glucose metabolism seem to be globally in agreement with that of typical cortical and subcortical AD pathology,[1,36–38] the hypometabolic area in the very mild stage of AD, PCC, was not consistent with the areas known to show the earliest pathologic abnormalities. PCC hypometabolism in the early stages of AD had been already suggested in several studies.[13,14] Moreover, studies on MCI have also reported that reduced glucose metabolism in PCC may differentiate MCI subjects who will progress to AD from those who will not.[39–41] In contrast to the findings from those functional imaging studies, neuropathologic or structural imaging studies for AD have revealed that the earliest changes in the AD brain begin at medial temporal areas, including entorhinal cortex and hippocampus.[1,42] This functional-structural discrepancy concerning involved anatomic regions (PCC vs. medial temporal area) in very mild AD may be explained in part by the following. PCC has anatomic connectivity with the parahippocampal and entorhinal regions according to a rhesus monkey study.[43] Neuronal loss in medial temporal areas possibly results in PCC hypometabolism, because glucose metabolism mainly reflects the activity of neuronal cell terminals rather than that of cell bodies.[5] One functional and structural imaging correlation study reported that direct correlation was detected between hippocampal gray matter density and posterior cingulate blood flow during a verbal recognition memory task in mild AD.[44] However, a recent study using a hippocampus mask indicated that the failure to detect hippocampal hypometabolism in many previous PET studies is probably because of a failed spatial alignment of relatively small structures like hippocampus in the

 

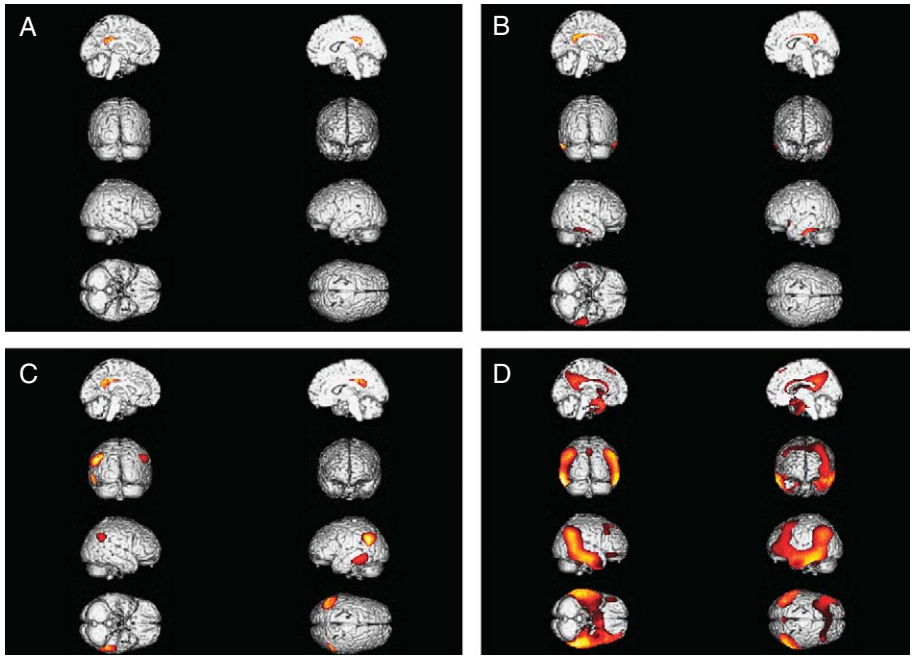


**FIGURE 1.** Brain areas of significant glucose metabolic reductions in (A) very mild AD (CDR 0.5); (B) mild AD (CDR 1); (C) moderate AD (CDR 2); (D) severe AD (CDR 3) compared with NC (CDR 0) ($P<0.001$, uncorrected for multiple comparison).

process of voxel-based analyses.[45] Therefore, further clarification for this issue should be made.

Significant correlations were found between clinical severity measure, CDR-SOB, and glucose metabolism in the PCC and bilateral inferior parietal lobule, indicating that regional metabolism in these areas could be used as a parameter to monitor disease progression from very mild to severe stage. These findings only partially coincide with those of Salmon et al's,[28] which showed the correlation between MMSE score and glucose metabolism in PCC and left precentral gyrus through voxel-based approach. This partial discrepancy might arise from the different clinical severity measure used in the 2 studies. Despite its popularity as a severity measure for dementia, however, MMSE has been criticized not only for its insensitivity to progressive changes occurring with severe AD (ie, floor effect), but also for its overemphasis on language-related left hemisphere function and relative insensitivity to the impairment of visuospatial ability-related right hemisphere function.[17] To avoid these limitations as a clinical severity measure, we used CDR or CDR-SOB, with no floor or hemispheric laterality effect, as a clinical severity measure.

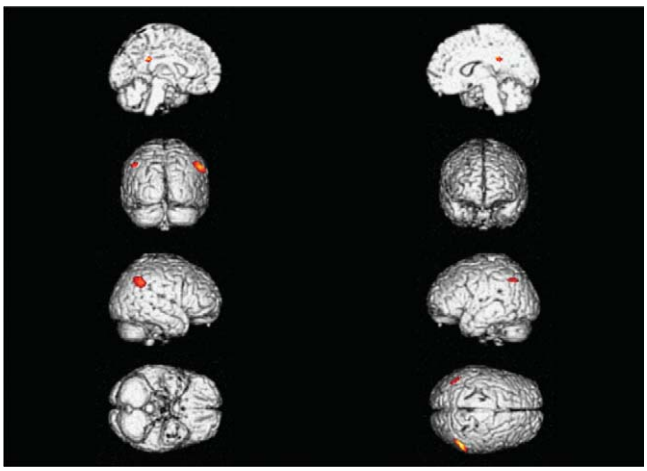

**FIGURE 2.** Brain areas with negative correlation between regional cerebral glucose metabolism and clinical severity (CDR-SOB) score under controlling age as a covariate ($P<0.005$, uncorrected for multiple comparison).

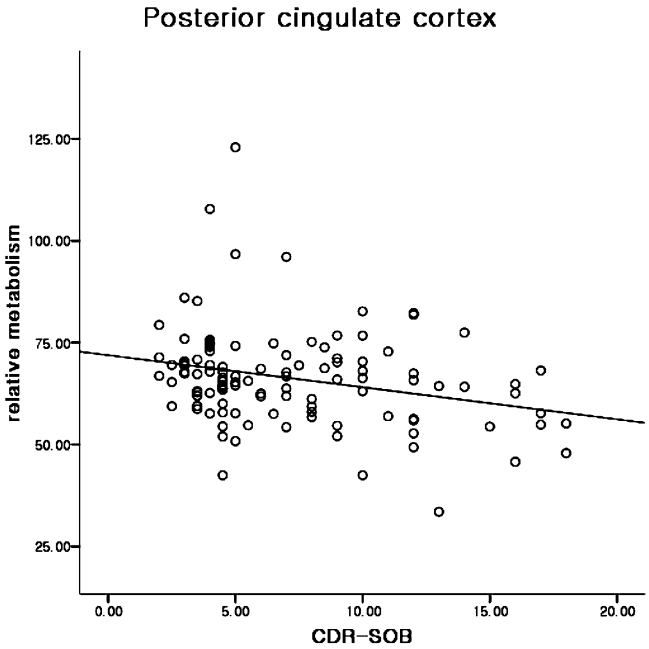


**FIGURE 3.** Illustration of the significant correlation obtained between clinical severity (CDR-SOB) and glucose metabolism in PCC region in AD.

Some possible limitations should be discussed. First, the numbers of subjects with severe stage of AD in the present study were not enough for sound statistical analyses. Therefore, cautious interpretation of results concerning comparisons between severe AD and other stage groups is needed. Second, we did not apply partial volume effect correction to PET data and regional hypometabolism of gray matter in AD might be overestimated. Although it was suggested that partial volume effect due to brain atrophy does not alter the general pattern of hypometabolism in overall AD patients, this effect should be considered in severe AD groups with relatively prominent brain atrophy.[46] Third, our study is not based on longitudinal follow-up, but only based on a cross-sectional observation. Therefore, we could provide little information about brain region-specific progression speed or amount of interval change, which is invaluable for the purpose of drug trials. A follow-up FDG-PET study for mild to moderate AD[47] provided the degree of region-specific metabolic decline over a 1-year interval and the estimated sample sizes for using FDG-PET as a drug efficacy parameter.

In conclusion, our results indicate that topographic patterns of brain dysfunction according to functional severity in AD are close to that of typical cortical and subcortical AD pathology, but that they do not fully coincide with it especially during very mild stage of the disease. In addition, cerebral glucose metabolism in the posterior cingulate and inferior parietal lobule can probably be used as a variable to monitor AD progression and as an early diagnostic marker of AD.

## REFERENCES


1. Braak H, Braak E. Neuropathological staging of Alzheimer-related changes. *Acta Neuropathol (Berl)*. 1991;82:239–259.
2. DeKosky ST, Scheff SW. Synapse loss in frontal cortex biopsies in Alzheimer's disease: correlation with cognitive severity. *Ann Neurol*. 1990;27:457–464.
3. Perry EK, Tomlinson BE, Blessed G, et al. Correlation of cholinergic abnormalities with senile plaques and mental test scores in senile dementia. *Br Med J*. 1978;2:1457–1459.
4. Terry RD, Masliah E, Salmon DP, et al. Physical basis of cognitive alterations in Alzheimer's disease: synapse loss is the major correlate of cognitive impairment. *Ann Neurol*. 1991;30:572–580.
5. Jueptner M, Weiller C. Dose measurement of regional cerebral blood flow reflect synaptic activity? Implications for PET and fMRI. *Neuroimage*. 1995;2:148–156.
6. Sokoloff L. Relationships among local functional activity, energy metabolism, and blood flow in the central nervous system. *Fed Proc*. 1981;40:2311–2316.
7. Duara R, Grady C, Haxby J, et al. Positron emission tomography in Alzheimer's disease. *Neurology*. 1986;36:879–887.
8. Herholz K, Salmon E, Perani D, et al. Discrimination between Alzheimer dementia and controls by automated analysis of multicenter FDG PET. *Neuroimage*. 2002;17:302–316.
9. Mentis MJ, Alexander GE, Krasuski J, et al. Increasing required neural response to expose abnormal brain function in mild versus moderate or severe Alzheimer's disease: PET study using parametric visual stimulation. *Am J Psychiatry*. 1998;155:785–794.
10. Mielke R, Herholz K, Grond M, et al. Differences of regional cerebral glucose metabolism between presenile and senile dementia of Alzheimer type. *Neurobiol Aging*. 1991;13:93–98.
11. Salmon E, Sadzot B, Maquet P, et al. Differential diagnosis of Alzheimer's disease with PET. *J Nucl Med*. 1994;35:391–398.
12. Pietrini P, Furey ML, Alexander GE, et al. Association between brain functional failure and dementia severity in Alzheimer's disease: resting versus stimulation PET study. *Am J Psychiatry*. 1999;156:470–473.
13. Ishii K, Mori T, Hirono N, et al. Glucose metabolic dysfunction in subjects with a clinical dementia rating of 0.5. *J Neurol Sci*. 2003;215:71–74.
14. Minoshima S, Giordani B, Berent S, et al. Metabolic reduction in the posterior cingulate cortex in very early Alzheimer's disease. *Ann Neurol*. 1997;42:85–94.
15. Nestor PJ, Fryer TD, Smielewski P, et al. Limbic hypometabolism in Alzheimer's disease and mild cognitive impairment. *Ann Neurol*. 2003;54:343–351.
16. Folstein MF, Folstein SE, McHugh PR. "Mini-Mental State": a practical method of grading the cognitive state of patients for the clinician. *J Psychiatr Res*. 1975;12:189–198.
17. Tombaugh TN, McIntrye NJ. The mini-mental state examination: a comprehensive review. *J Am Geriatr Soc*. 1992;40:922–935.
18. Hughes CP, Berg L, Danziger W, et al. A new clinical scale for the staging of dementia. *Br J Psychiatry*. 1982;140:566–572.
19. American Psychiatric Association. *Diagnostic and Statistical Manual of Mental Disorders*. 4th ed. Washington, DC: American Psychiatric Association; 1994.
20. Mckhann G, Drachman D, Folstein M, et al. Clinical diagnosis of Alzheimer's disease: report of the NINCDS-ADRDA work group under the auspices of Department of Health and Human Services Task force on Alzheimer's disease. *Neurology*. 1984;34:939–944.
21. Lee JH, Lee KU, Lee DY, et al. Development of the Korean version of the Consortium to Establish a Registry for Alzheimer's Disease Assessment Packet (CERAD-K): clinical and neuropsychological assessment battery. *J Gerontol Psychol Sci*. 2002;57:47–53.
22. Morris JC, Heyman A, Mohs RC, et al. The Consortium to Establish a Registry for Alzheimer's Disease (CERAD). Part I. Clinical and neuropsychological assessment of Alzheimer's disease. *Neurology*. 1989;39:1159–1165.
23. Morris JC. The Clinical Dementia Rating (CDR): current version and scoring rules. *Neurology*. 1993;43:2412–2414.
24. Minoshima S, Frey KA, Foster NL, et al. Preserved pontine glucose metabolism in Alzheimer disease: a reference region for functional brain image (PET) analysis. *J Comput Assist Tomogr*. 1995;19:541–547.
25. Friston KJ, Holmes AP, Worsley KJ, et al. Statistical parametric maps in functional imaging: a general linear approach. *Hum Brain Mapp*. 1995;2:189–210.
26. Friston KJ, Frith CD, Liddle PF, et al. Comparing functional (PET) images: the assessment of significant change. *J Cereb Blood Flow Metab*. 1991;11:690–699.
27. Forman SD, Cohen JD, Fitzgerald M, et al. Improved assessment of significant activation in functional magnetic resonance imaging (fMRI): use of a cluster-sized threshold. *Mag Res Med*. 1995;33:636–647.
28. Salmon E, Collette F, Degueldre C, et al. Voxel-based analysis of confounding effects age and dementia severity on cerebral metabolism in Alzheimer's disease. *Hum Brain Mapp*. 2000;10:39–48.
29. Garraux G, Salmon E, Degueldre C, et al. Comparison of impaired subcortico-frontal metabolic networks in normal aging, subcortical-frontal dementia, and cortical frontal dementia. *Neuroimage*. 1999;10:149–162.
30. Petit-Taboué MC, Landeau B, Desson JF, et al. Effects of healthy aging on the regional cerebral metabolic rate of glucose assessed with statistical parametric mapping. *Neuroimage*. 1998;7:176–184.
31. Talairach J, Tournoux P. *Co-planar Stereotaxic Altlas of the Human Brain*. New York: Thieme; 1988.
32. Lee DY, Lee KU, Lee JH, et al. A normative study of the CERAD neuropsychological assessment battery in the Korean elderly. *J Int Neuropsychol Soc*. 2004;10:72–81.
33. Haxby JV, Grady CL, Koss E, et al. Heterogeneous anterior-posterior metabolic patterns in dementia of the Alzheimer type. *Neurology*. 1988;38:1853–1863.


 

34. Kim EJ, Cho SS, Jeong Y, et al. Glucose metabolism in early onset versus late onset Alzheimer's disease: an SPM analysis of 120 patients. *Brain*. 2005;128:1790–1801.
35. Callen DJA, Black SE, Gao F, et al. Beyond the hippocampus: MRI volumetry confirms widespread limbic atrophy in AD. *Neurology*. 2001;57:1669–1674.
36. Paskavitz JF, Drachman DA, Hamos JE. Alterations in the dorsomedial nucleus of the thalamus in Alzheimer's disease. *Neurology*. 1990;20(suppl 1):339.
37. Pearce BR, Palmer AM, Bowen DM, et al. Neurotransmitter dysfunction and atrophy of the caudate nucleus in Alzheimer's disease. *Neurochem Pathol*. 1984;2:221–232.
38. Tiraboschi P, Hansen LA, Thal LJ, et al. The importance of neuritic plaques and tangles to the development and evolution of AD. *Neurology*. 2004;62:1984–1989.
39. Chételat G, Desgranges B, de la Sayette V, et al. Mild cognitive impairment: Can FDG-PET predict who is to rapidly convert to Alzheimer's disease? *Neurology*. 2003;60: 1374–1377.
40. Huang C, Wahlund LO, Almkvist O, et al. Cingulate cortex hypoperfusion predicts Alzheimer's disease in mild cognitive impairment. *BMC Neurol*. 2002;2:1–6.
41. Mosconi L, Perani D, Sorbi S, et al. MCI conversion to dementia and the APOE genotype. A prediction study with FDG-PET. *Neurology*. 2004;63:2332–2340.
42. Dickerson BC, Goncharova I, Sullivan MP, et al. MRI-based entorhinal and hippocampal atrophy in incipient and very mild Alzheimer's disease. *Neurobiol Aging*. 2001;22:747–754.
43. Morris R, Petrides M, Pandya DN. Architecture and connections of retrosplenial area 30 in the rhesus monkey (macaca mulatta). *Eur J Neurosci*. 1999;11:2506–2518.
44. Garrido GEJ, Furuie SS, Buchpiguel CA, et al. Relation between medial temporal atrophy and functional brain activity during memory processing in Alzheimer's disease: a combined MRI and SPECT study. *J Neurol Neurosurg Psychiatry*. 2002;73:508–516.
45. Mosconi L, Tsui WH, De Santi S, et al. Reduced hippocampal metabolism in MCI and AD. *Neurology*. 2005;64:1860–1867.
46. Ibanez V, Pietrini P, Alexander GE, et al. Regional glucose metabolic abnormalities are not the result of atrophy in Alzheimer's disease. *Neurology*. 1998;50:1585–1593.
47. Alexander GE, Chen K, Pietrini P, et al. Longitudinal PET evaluation of cerebral metabolic decline in Dementia: a potential outcome measure in Alzheimer's disease treatment studies. *Am J Psychiatry*. 2002;159:738–745.